AD NUMBER
ADB254502
NEW LIMITATION CHANGE

TO

Approved for public release, distribution unlimited

FROM

Distribution authorized to U.S. Gov't. agencies only; Proprietary Info; Sep 99 Other requests shall be referred to USAMRMC, Fort Detrick, MD 21702-5012

AUTHORITY

U.S. Army Medical Research and Materiel Command and Fort Detrick ltr., dtd October 17, 2001.

AD _____

Award Number: DAMD17-97-1-7045

TITLE: Vascular CD44 Expression and Breast Cancer Angiogenesis and Metastasis

PRINCIPAL INVESTIGATOR: Kristina Flores
Laura P. Hale, Ph.D.

CONTRACTING ORGANIZATION: Duke University Medical Center
Durham, North Carolina 27710

REPORT DATE: September 1999

TYPE OF REPORT: Annual

PREPARED FOR: U.S. Army Medical Research and Materiel Command
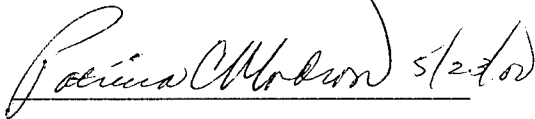Fort Detrick, Maryland 21702-5012

20000607 065

NOTICE

USING GOVERNMENT DRAWINGS, SPECIFICATIONS, OR OTHER DATA INCLUDED IN THIS DOCUMENT FOR ANY PURPOSE OTHER THAN GOVERNMENT PROCUREMENT DOES NOT IN ANY WAY OBLIGATE THE U.S. GOVERNMENT. THE FACT THAT THE GOVERNMENT FORMULATED OR SUPPLIED THE DRAWINGS, SPECIFICATIONS, OR OTHER DATA DOES NOT LICENSE THE HOLDER OR ANY OTHER PERSON OR CORPORATION; OR CONVEY ANY RIGHTS OR PERMISSION TO MANUFACTURE, USE, OR SELL ANY PATENTED INVENTION THAT MAY RELATE TO THEM.

LIMITED RIGHTS LEGEND

Award Number: DAMD17-97-1-7045
Organization: Duke University Medical Center
Location of Limited Rights Data (Pages):

Those portions of the technical data contained in this report marked as limited rights data shall not, without the written permission of the above contractor, be (a) released or disclosed outside the government, (b) used by the Government for manufacture or, in the case of computer software documentation, for preparing the same or similar computer software, or (c) used by a party other than the Government, except that the Government may release or disclose technical data to persons outside the Government, or permit the use of technical data by such persons, if (i) such release, disclosure, or use is necessary for emergency repair or overhaul or (ii) is a release or disclosure of technical data (other than detailed manufacturing or process data) to, or use of such data by, a foreign government that is in the interest of the Government and is required for evaluational or informational purposes, provided in either case that such release, disclosure or use is made subject to a prohibition that the person to whom the data is released or disclosed may not further use, release or disclose such data, and the contractor or subcontractor or subcontractor asserting the restriction is notified of such release, disclosure or use. This legend, together with the indications of the portions of this data which are subject to such limitations, shall be included on any reproduction hereof which includes any part of the portions subject to such limitations.

THIS TECHNICAL REPORT HAS BEEN REVIEWED AND IS APPROVED FOR PUBLICATION.

REPORT DOCUMENTATION PAGE

Form Approved
OMB No. 074-0188

1. AGENCY USE ONLY (Leave blank)	2. REPORT DATE September 1999	3. REPORT TYPE AND DATES COVERED Annual (15 Aug 98 -14 Aug 99)

4. TITLE AND SUBTITLE Vascular CD44 Expression and Breast Cancer Angiogenesis and Metastasis	5. FUNDING NUMBERS DAMD17-97-1-7045

6. AUTHOR(S)
Kristina Flores

Laura P. Hale, Ph.D.

7. PERFORMING ORGANIZATION NAME(S) AND ADDRESS(ES)
Duke University Medical Center
Durham, North Carolina 27710

e-mail:
krg4@acpub.duke.edu

8. PERFORMING ORGANIZATION REPORT NUMBER

9. SPONSORING / MONITORING AGENCY NAME(S) AND ADDRESS(ES)

U.S. Army Medical Research and Materiel Command
Fort Detrick, Maryland 21702-5012

10. SPONSORING / MONITORING AGENCY REPORT NUMBER

11. SUPPLEMENTARY NOTES

12a. DISTRIBUTION / AVAILABILITY STATEMENT
Distribution authorized to U.S. Government agencies only (proprietary information, September 1999). Other requests for this document shall be referred to U.S. Army Medical Research and Materiel Command, 504 Scott Street, Fort Detrick, Maryland 21702-5012.

12b. DISTRIBUTION CODE

13. ABSTRACT (Maximum 200 Words)

The breast cancer susceptibility gene, BRCA2, has been shown to play a role in cellular proliferation, differentiation and DNA repair. Several lines of evidence suggest that the double stranded DNA repair process that occurs normally in the thymus during T-cell receptor gene rearrangement may provide a good model for studying BRCA2 function. First, whereas BRCA2 is expressed at relatively low levels in most tissues, it is highly expressed in normal thymus, a tissue having elevated levels of proliferation, differentiation and DNA breakage and repair compared to other tissues. Second, mice carrying a truncating mutation in the 5' region of BRCA2 exon 11 often develop thymic lymphomas that may be the result of defects in DNA repair in the thymus. Furthermore, embryonic fibroblasts from these mice have an impaired ability to repair double stranded DNA breaks after X-irradiation. Finally, BRCA2 has been shown to bind to RAD51, the eukaryotic RecA homologue known to function in double stranded DNA repair. In this study, we have analyzed BRCA2 expression in thymocyte subsets and we have developed assays to test the ability of BRCA2 to function in double stranded DNA repair during gene rearrangement in cells with modified BRCA2 expression.

14. SUBJECT TERMS Breast Cancer, Predoc Award			15. NUMBER OF PAGES 58
			16. PRICE CODE

17. SECURITY CLASSIFICATION OF REPORT Unclassified	18. SECURITY CLASSIFICATION OF THIS PAGE Unclassified	19. SECURITY CLASSIFICATION OF ABSTRACT Unclassified	20. LIMITATION OF ABSTRACT Unlimited

NSN 7540-01-280-5500

Standard Form 298 (Rev. 2-89)
Prescribed by ANSI Std. Z39-18
298-102

FOREWORD

Opinions, interpretations, conclusions and recommendations are those of the author and are not necessarily endorsed by the U.S. Army.

_____ Where copyrighted material is quoted, permission has been obtained to use such material.

_____ Where material from documents designated for limited distribution is quoted, permission has been obtained to use the material.

_KT____ Citations of commercial organizations and trade names in this report do not constitute an official Department of Army endorsement or approval of the products or services of these organizations.

_✓_ In conducting research using animals, the investigator(s) adhered to the "Guide for the Care and Use of Laboratory Animals," prepared by the Committee on Care and use of Laboratory Animals of the Institute of Laboratory Resources, national Research Council (NIH Publication No. 86-23, Revised 1985).

_KT_✓_ For the protection of human subjects, the investigator(s) adhered to policies of applicable Federal Law 45 CFR 46.

_KT_NA_ In conducting research utilizing recombinant DNA technology, the investigator(s) adhered to current guidelines promulgated by the National Institutes of Health.

_KT_NA_ In the conduct of research utilizing recombinant DNA, the investigator(s) adhered to the NIH Guidelines for Research Involving Recombinant DNA Molecules.

_KT_NA_ In the conduct of research involving hazardous organisms, the investigator(s) adhered to the CDC-NIH Guide for Biosafety in Microbiological and Biomedical Laboratories.

Kristina A Hous 9-13-99
PI - Signature   Date

Table of Contents

Introduction

The breast cancer susceptibility gene, BRCA2, has been shown to play a role in cellular proliferation, differentiation and DNA repair. Several lines of evidence suggest that the double stranded DNA repair process that occurs normally in the thymus during T-cell receptor (TCR) gene rearrangement may provide a good model for studying BRCA2 function. First, whereas BRCA2 is expressed at relatively low levels in most tissues, it is highly expressed in normal thymus, a tissue having elevated levels of proliferation, differentiation and DNA break and repair compared to other tissues [1]. Second, mice carrying a truncating mutation in the 5' region of BRCA2 exon 11 often develop thymic lymphomas that may be the result of defects in DNA repair in the thymus. Furthermore, embryonic fibroblasts from these mice have an impaired ability to repair double stranded DNA breaks after X-irradiation [2, 3]. Finally, BRCA2 has been shown to bind to RAD51, the eukaryotic RecA homologue known to be involved in double stranded DNA repair [4-7]. This evidence suggests that BRCA2 plays an important role in double stranded DNA repair, particularly in T-cell receptor gene rearrangement within the thymus. In this study, we have developed assays to test the ability of BRCA2 to function in T-cell receptor gene rearrangement in cells with decreased BRCA2 expression and have analyzed BRCA2 expression in thymocyte subsets. These studies suggest that BRCA2 plays a role in thymocyte development. This model system may be useful for studying the role of BRCA2 in DNA repair.

BODY

The specific aims of this work are as follows:

1) **Develop dynamic *in vitro* assays to measure T-cell receptor gene rearrangement :**

a. Develop methods to detect DNA double stranded breaks as a function of T-cell receptor gene rearrangement by optimizing Ligation Mediated -Polymerase Chain Reaction (LM-PCR) in primary human thymocytes.

b. Develop a recombination substrate assay to test T-cell receptor gene rearrangement in human cell lines in which BRCA2 levels can be modulated.

2) **Determine the effects of under- and over-expression of BRCA2 on T-cell receptor gene rearrangement as a model for general processes of DNA breakage and repair.**

a. Modulate BRCA2 using a panel of BRCA2 sense and antisense expression vectors and/or antisense oligonucleotides.

b. Measure effects of BRCA2 under- and over-expression on T-cell receptor gene rearrangement using LM-PCR or recombination substrate assays developed in objective one.

Results

Objective 1a. Develop methods to detect DNA double stranded breaks as a function of T-cell receptor gene rearrangement by optimizing Ligation Mediated - PCR (LM-PCR) in primary human thymocytes.

The LM-PCR assay described previously was used to detect rearrangements occurring 5' or 3' to the Dβ 2.1 human locus. The Dβ probe detects a 503 bp band corresponding to a D-J gene segment rearrangement and a 422 bp band corresponding to a V-DJ gene segment rearrangement. The rearrangement signals at bp 503 and 422, indicative of TCR β chain rearrangement, are consistently present in pediatric thymocytes. Since the last report, we have analyzed 14 pediatric thymus samples and have found signals corresponding to D-J and V-DJ TCR β chain gene rearrangement in all pediatric samples. We have also analyzed 8 adult thymus tissues and found D-J TCR gene rearrangement in 8 of the 8 adult thymus tissues and V-DJ signals in 5 of the 8 adult thymus tissues.

LM-PCR has thus far not been used in studies regarding BRCA2 and TCR gene rearrangement as we have encountered difficulties transfecting primary thymocytes (maximum efficiency >3%). However, the use of LM-PCR to analyze human thymocytes has been extremely beneficial for studies regarding changes in the human thymic perivascular space during aging. A recent manuscript regarding the human thymic perivascular space during aging is now in press. (See manuscript Flores et. al) This study may be critical to understanding the factors which lead to thymic aging and lead to advances in immune reconstitution of breast cancer patients undergoing high dose chemotherapy followed by bone marrow transplantation.

1b. Develop a recombination substrate assay to test T-cell receptor gene rearrangement in human cell lines in which BRCA2 levels can be modulated.

<u>Recombination Assays Using A Novel Recombinaiton Substrate</u> In the last report, we described strategies to generate and test a novel recombination substrate based the expression of green fluorescent protein (GFP). The GFP-based recombination substrate was co-transfected into 293T and breast cancer cells along with recombination activating

genes (rag) rag-1 and rag-2 under conditions that have previously been shown to be sufficient for TCR-type recombination of similarly designed substrates in fibroblasts and other non-lymphocyte systems. After 48 hours, the cells were analyzed for recombination by two methods. First, the number of cells with correctly rearranged recombination substrates and expressing GFP was measured by flow cytometry. We detected only slight increases in fluorescence ($\leq 1\%$) in cells transfected with the GFP recombination substrate and rag-1 and rag-2 proteins. Upon repeated studies and further examination, it was not clear if a 1% recombination efficiency could be accurately detected by flow cytometry since the mean fluorescence values of all samples remained relatively equal. We then extracted low molecular weight DNA from transfected cells and analyzed for the presence of correctly rearranged GFP by PCR using GFP-specific primers. Recombination was predicted to result in a band of 267 bp versus 1200 bp for unrearranged GFP. All samples tested by PCR with GFP specific primers resulted in a "ladder" of products that were all reactive with a specific GFP radiolabled probe after Southern Blot analysis (data not shown). This result led us to hypothesize that the recombination substrate was being degraded once inside the cell.

The Novel Recombination Substrate, GpG-5-2 During this time we began a collaboration with Dr. Rachel Gerstein at the University of Massachusetts. Dr. Gerstein has generated a similar GFP-based recombination substrate. This recombination substrate is based on inversional recombination which allows a full length GFP protein sequence to be inverted within a locus and placed near a promoter sequence. It is only after inversion takes place that the start site of GFP is close enough to the promoter to allow proper transcription and translation of the GFP protein. Dr. Gerstein's construct is contained in a pseudo-typed vesicular stomatitis virus that infects cells at a high efficiency and contains an antibiotic resistance gene for selection of infected cells using blasticidin S. We have tested this construct, named GpG-5-2, in DR3 cells and in Capan-1 (BRCA2 truncated) cells using flow cytometry and nested PCR.

We found that GpG-5-2 infects DR3 cells at a high efficiency (40 -85%). A control construct similar to GpG-5-2 contains functional GFP that is expressed after infection of the cell and allows quantification of infection efficiencies by flow cytometry. Cells infected with GpG-5-2 were then selected with blasticidin S to generate a pure population of cells containing GpG-5-2.

DR3 cells contain rag-1 and rag-2 under the control of a heat shock inducible promoter. These cells also express rag-1 and rag-2 proteins constitutively at very low levels. Even with only baseline rag expression, almost 83% of DR3 cells infected with

GpG-5-2 were found to express GFP by flow cytometry 72 hours after initial infection. GpG-5-2 recombination was confirmed in these cells by nested PCR using construct specific primers and a reverse primer specific to a rearrangement junction (see Figure 1).

BRCA2 truncated Capan-1 cells were also infected with GpG-5-2 and transfected with rag constructs as described above. Although recombination can be detected in cells by PCR, flow cytometry results suggest that only 1-3% percent of cells have received the constructs and have rearranged the recombination substrate. The lower recombination efficiency in Capan-1 cells compared to DR3 cells is most likely due to the limited transfection efficiency of Capan-1 cells. The highest transfection efficiency achieved using traditional methods has been 7% in Capan-1 cells.

We will continue to use this recombination substrate in Capan-1 and other cells to determine if modulating BRCA2 using our full length BRCA2 antisense construct has an effect on the recombination efficiency of GpG-5-2.

Objective 2a. Modulate BRCA2 using a panel of BRCA2 sense and antisense expression vectors and/or antisense oligonucleotides.

2b. Measure effects of BRCA2 under- and over-expression on T-cell receptor gene rearrangement using LM-PCR or recombination substrate assays developed in objective 1.

<u>BRCA2 Expression Constructs</u> As stated in the last report, our lab has generated full length BRCA2 expression constructs and several BRCA2 antisense expression vectors and oligonucleotides. The full length BRCA2 antisense construct has been used to decrease BRCA2 RNA levels in 293T cells (see Figure 2). However, it will be necessary to use BRCA2 antisense constructs in Capan-1 cells and other cells which have been successfully used in the recombination substrate assay since we have not been able to determine if the recombination substrate undergoes rearrangement successfully upon infection into 293T cells.

As shown above, DR3 cells have a high recombination efficiency of the GFP recombination substrate as measured by flow cytometry and PCR. Thus far, all experiments have been targeted for use in human cell lines. However, DR3 cells, obtained from a murine B-cell lymphoma, may be the most useful in determining if BRCA2 plays a role in TCR gene rearrangement. Future studies will include the generation of mouse BRCA2 antisense oligonucleotides to decrease BRCA2 expression in DR3 cells and to test the effects of BRCA2 modulation in the recombination substrate assay.

BRCA2 Expression   An additional aim regarding BRCA2 expression in thymocyte subsets has provided useful information which suggests that BRCA2 is necessary for thymocyte development. High levels of BRCA2 RNA were found to be associated with whole thymus compared to thymic stroma consisting of epithelial cells, fibroblasts and macrophages (data not shown). The majority of the BRCA2 RNA found in whole thymus was further localized to the thymocytes by study of RNA expression. This study suggested that thymocytes, in particular, express BRCA2 RNA versus other thymic cells including epithelial cells, macrophages and fibroblasts contained in the thymic stroma. No BRCA2 RNA was detectable in thymic stroma by Northern Blot analysis under equal loading conditions.

Using RT-PCR, we have determined that BRCA2 mRNA is expressed in thymocyte subsets in which β chain (CD4$^-$ CD8$^-$ CD3$^-$ triple negative thymocytes) and α chain rearrangement (CD4$^+$ CD8$^+$ double positive thymocytes) occur. These studies support the hypothesis that BRCA2 has a role in TCR gene rearrangement Additional RT-PCR studies to analyze BRCA2 expression in thymocyte subsets have revealed that BRCA2 is expressed at higher levels in immature CD4$^+$ CD8$^+$ double positive thymocytes compared to more mature single positive CD4$^+$ or CD8$^+$ thymocytes (see Figure 3). The difference in BRCA2 expression has been confirmed by quantitative PCR using the new Light Cycler RT-PCR system from Roche Molecular Biochemicals (see Table 1). These studies suggest that BRCA2 plays a role in thymocyte development and perhaps specifically in TCR gene rearrangement.

Summary

In support of our aims regarding the function of BRCA2 in TCR gene rearrangement, we have generated a GFP-based recombination substrate assay in collaboration with Dr. Rachel Gerstein at the University of Massachusetts. Additional studies to modify BRCA2 expression in cells have also been successful and we are currently testing the effects of decreased BRCA2 expression in cells using the GFP-based recombination substrate assay. Our studies showing that BRCA2 is highly expressed in immature thymocyte subsets suggest that BRCA2 has a role in thymocyte development to some degree. Finally, we have used the LM-PCR assay for additional studies regarding changes in the human thymic perivascular space during aging which has resulted in a manuscript in press.

1. Rajan, J.V., *et al.*, *Brca2 is coordinately regulated with Brca1 during proliferation and differentiation in mammary epithelial cells.* Proc Natl Acad Sci U S A, 1996. **93**(23): p. 13078-83.

2. Connor, F., *et al.*, *Tumorigenesis and a DNA repair defect in mice with a truncating Brca2 mutation.* Nat Genet, 1997. **17**(4): p. 423-30.

3. Friedman, L.S., *et al.*, *Thymic lymphomas in mice with a truncating mutation in Brca2.* Cancer Res, 1998. **58**(7): p. 1338-43.

4. Chen, J.-J., *et al.*, *Brca1, Brca2, and Rad 51 operate in a common DNA damage response pathway.* Cancer Research, 1999. **59**: p. 1752s-1756s.

5. Katagiri, T., *et al.*, *Multiple possible sites of BRCA2 interacting with DNA repair protein RAD51.* Genes Chromosomes Cancer, 1998. **21**(3): p. 217-22.

6. Mizuta, R., *et al.*, *RAB22 and RAB163/mouse BRCA2: proteins that specifically interact with the RAD51 protein.* Proc Natl Acad Sci U S A, 1997. **94**(13): p. 6927-32.

7. Sharan, S.K., *et al.*, *Embryonic lethality and radiation hypersensitivity mediated by Rad51 in mice lacking Brca2 [see comments].* Nature, 1997. **386**(6627): p. 804-10.
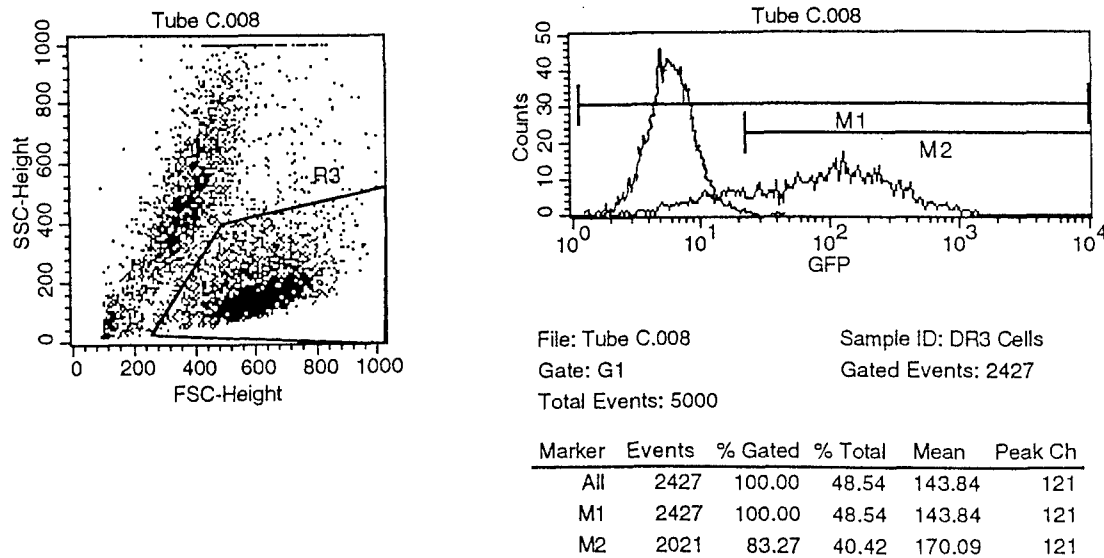
File: Tube C.008   Sample ID: DR3 Cells
Gate: G1   Gated Events: 2427
Total Events: 5000

Marker	Events	% Gated	% Total	Mean	Peak Ch
All	2427	100.00	48.54	143.84	121
M1	2427	100.00	48.54	143.84	121
M2	2021	83.27	40.42	170.09	121

Figure 1. DR3 cells express GFP after recombination of GpG-5-2. DR3 cells infected with the recombination substrate, GpG-5-2, rearrange the GFP reporter gene and express GFP at high levels (M2=83.27%) versus DR3 cells that are not infected with GpG-5-2 (M2=0.27%)
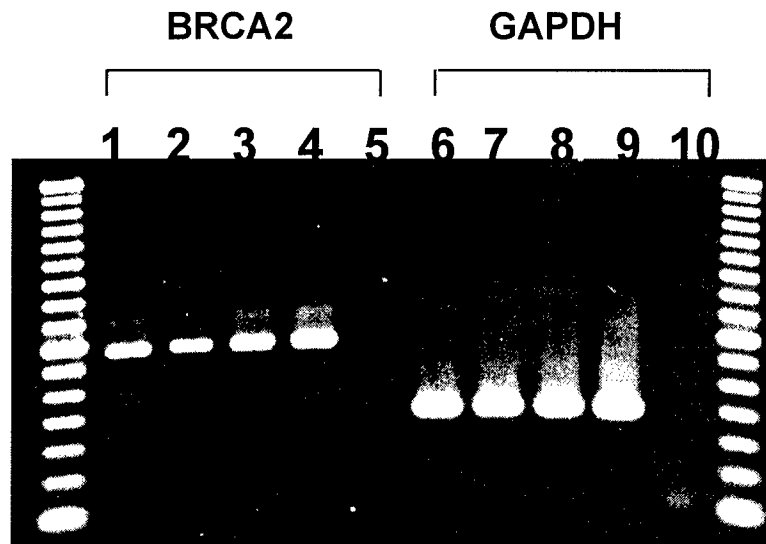
11

Figure 2. BRCA2 is Detected in Thymocyte Subsets by RT-PCR. Normal human thymocytes from a pediatric patient were reacted with directly labeled CD4 and CD8 mAbs, then sorted by flow cytometry to isolate double positive (CD4$^+$ CD8$^+$) and single positive (CD4$^+$CD8$^-$ or CD4$^-$CD8$^+$) thymocytes. RNA from each subset was used for RT-PCR reactions with BRCA2 or GAPDH primers for 35 cycles. Lane 1 and 6= CD4$^+$ CD8$^-$, lane 2 and 7 = CD4$^-$ CD8$^+$, lane 3 and 8 = CD4$^+$CD8$^+$, lane 4 and 9 =MCF7 breast cancer cells. Primers specific for BRCA2 and GAPDH amplify a 323 bp product and a 190 bp product respectively from 2 μl each cDNA. Lanes 5 and 10 are PCR controls. Specific bands corresponding to BRCA2 were seen in each thymocyte subset examined. The strongest signals were seen in double positive thymocyte subsets (lane 3) compared to single positive subsets (lanes 1 and 2) whereas GAPDH signals are strong in all samples.

BRCA2 cDNA   +   -   +

BRCA2 Antisense   -   +   +
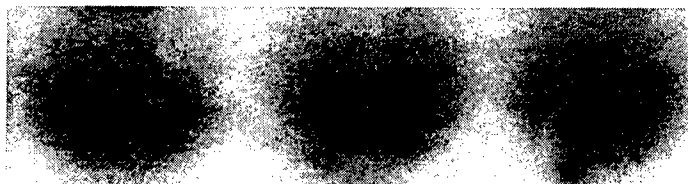

BRCA2
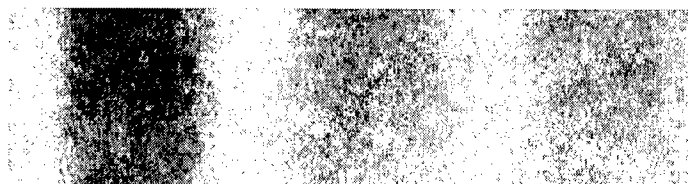
GAPDH

Figure 3. BRCA2 Full Length Antisense Decreases BRCA2 Message by Northern Blot Analysis. 293T cells transfected with a full length BRCA2 antisense construct have decreased BRCA2 RNA levels when normalized against GAPDH RNA levels.

Thymocyte Subset	Concentration (ng/μl)
CD4$^+$ single positive	27.80
CD8$^+$ single positive	38.18
CD4$^+$ CD8$^+$ double positive	70.05

Table 1. BRCA2 expression is increased in immature double positive thymocyte subsets. Single positive (CD4$^+$ or CD8$^+$) and double positive (CD4$^+$ CD8$^+$) thymocyte subsets were analyzed for BRCA2 expression using the RT-PCR Light Cycler system from Roche Molecular Biochemicals. The Light Cycler system allows for real time quantitative PCR by measuring the fluorescence incorporation of SYBR Green I dye which binds to double stranded DNA. Values are calculated using a standard curve of known concentrations of DNA equalized from a previous reaction using GAPDH primers.

Key Research Accomplishments

- Development of *in vitro* assays to test the function of BRCA2 in TCR gene rearrangement including:
    - Ligation Mediated PCR
    - GFP-based Recombination Substrate Assay

- BRCA2 was found to be highly expressed in immature $CD4^+$ $CD8^+$ double positive thymocyte subsets.

- BRCA2 expression was found to be decreased in cells transfected with BRCA2 antisense constructs.

Reportable Outcomes

Manuscript: Flores et. al, 1999; Analysis of the Human Thymic Perivascular Space During Aging

Presentations: Analysis of the Human Thymic perivascular Space During Aging; Society for the Advancement of Chicanos and Native Americans in Science (SACNAS) Conference 1999, October 7-11, Portland, Oregon. Abstract submitted

Analysis of the Human Thymic Perivascular Space During Aging

By Kristina G. Flores, Jie Li, Gregory D. Sempowski*[+], Barton F. Haynes*[+], and Laura P. Hale

Departments of Pathology, Medicine*, and Immunology[+]
Duke University Medical Center, Durham, NC

Running title: Changes in Thymic PVS with Aging

Correspondence to:
Laura P. Hale, M.D. Ph.D.
DUMC 2608
185 Medical Sciences Research Building
Duke University Medical Center
Durham, NC 27710
Phone (919) 684-4771
FAX   (919) 684-8756
Email: hale0004@mc.duke.edu

Acknowledgments

Abstract

The perivascular space of human thymus increases in volume during aging as thymopoiesis declines. Understanding the composition of the perivascular space is thus vital to understanding mechanisms of thymic atrophy. We have analyzed 87 normal and 31 myasthenia gravis thymus tissues from newborn to 78 years using immunohistologic and molecular assays. We confirmed that although thymic epithelial space volume decreases progressively with age, thymopoiesis with active T-cell receptor gene rearrangement continued normally within the thymic epithelial space into late life. Hematopoietic cells present in the adult perivascular space include T-cells, B cells, and monocytes. Eosinophils are prominent in perivascular space of infants $\leq$ age 2. Perivascular space of both normal adult and myasthenia gravis thymus contains mature single positive (CD1a$^-$, CD4$^+$ or CD8$^+$) T lymphocytes that express CD45RO, including clusters of T-cells expressing the TIA-1 cytotoxic granule antigen, suggesting a peripheral origin. Peripheral blood mononuclear cells bind *in vitro* to MECA-79$^+$ high endothelial venules present in the perivascular space, suggesting a mechanism for the recruitment of peripheral cells to thymic perivascular space. Thus in both normal subjects and myasthenia gravis patients, thymic perivascular space may be a compartment of the peripheral immune system that is not directly involved in thymopoiesis.

Keywords: thymus, aging, perivascular space, myasthenia gravis, lymphocyte homing

Introduction

The human thymic cortex contains densely packed immature thymocyte precursors within a thymic epithelial framework and, in children, is located directly beneath the thymic capsule. The thymic medulla is distinguished histologically by its less dense arrangement of thymocytes and by the presence of concentric whorls of keratin and terminally differentiated thymic epithelial cells termed Hassall's bodies. The thymic cortex and medulla together comprise the thymic epithelial space (TES) where thymopoiesis occurs. Recent studies have focused attention on a third anatomic region of the thymus, termed the perivascular space (PVS) (1, 2), for its location adjacent to the blood vessels. The PVS is located within the thymic capsule but is separated from the TES by a basement membrane and does not contain developing thymocytes (3, 4, 5). Early in life, the thymus is composed primarily of TES that supports thymopoiesis and generation of the peripheral T-cell repertoire. As the thymus ages, the TES begins to atrophy while the PVS increases in size as it fills with adipose tissue and lymphoid cells (2). However, the origin of cells within the thymic PVS, as well as the role of the thymic PVS in the process of thymic atrophy are unclear. Steinmann and Hartwig have postulated that cytotoxic T lymphocytes (CTL) migrating back to the thymus target medullary thymic epithelial cells expressing mutated self peptides that accumulate over time and thus induce loss of thymic stroma leading to thymic atrophy (6). For this hypothesis to be plausible, mature CTL should be identifiable within the thymic medulla of normal thymus tissue undergoing age-related atrophy.

In this paper, we study the PVS in aging normal and myasthenia gravis human thymuses. We describe age-related changes in PVS cellular composition and demonstrate

the mature phenotype of the T-cells present in the PVS, including a population of cytotoxic granule-containing cells with the phenotype of mature CTL.

Materials and Methods

Cell and Tissues:

Human thymus tissues were obtained as discarded tissue at the time of necessary cardiothoracic surgery or after thymectomy for the treatment of myasthenia gravis (MG), according to an Institutional Review Board-approved protocol for the use of discarded tissues. Tissues with thymoma were excluded. Portions of each tissue were fixed in 10% neutral buffered formalin for 6-24 hours, then processed into paraffin blocks using standard histologic procedures. Additional portions of most tissues were snap-frozen and stored at or below –80°C until used. Formalin-fixed paraffin-embedded (FFPE) sections were used whenever possible to facilitate good histologic sampling of all tissue compartments. Thymus tissues were also obtained from the archives of the Duke University Department of Pathology as FFPE sections. All tissues were used anonymously, with recording of only patient age, gender, and surgical diagnosis. Table 1 describes the clinical characteristics of the patients from whom thymic tissue was obtained. Peripheral blood mononuclear cells (PBMC) for high endothelial venule binding assays were obtained from human blood by density gradient centrifugation (Lymphocyte Separation Medium, ICN Biomedicals Inc.).

Antibodies

The following monoclonal and polyclonal antibodies were used: anti-cytokeratin (cocktail of AE1/AE3, Boehringer Mannheim, Indianapolis, IN; plus CAM5.2, Becton Dickinson, San Jose, CA), CD1a (O10, kind gift of L. Boumsell) (7), CD3 (rabbit polyclonal #A0452, Dako, Carpinteria, CA) (8), CD4 (1F6, Novo Castra, Newcastle upon Tyne, UK), CD8 (C8/144B, Dako), CD20 (L26, Dako), CD38 (T16, Beckman Coulter; AT13/5, Harlan Bioproducts, Indianapolis), CD45RA (HI115; obtained through the 6th International Workshop on Leukocyte Differentiation Antigens), CD45RO (UCHL-1, American Type Culture Collection, Rockville, MD), CD68 (KP-1, Dako), Ki-67 nuclear proliferation antigen (mib-1, Beckman Coulter) (9), anti-cytotoxic granule protein (TIA-1, Beckman Coulter) (10), anti-perivascular space (TE-7) (11), anti-high endothelial venule (MECA-79 and MECA-367, kind gift of E. Butcher) (12, 13). Isotype matched control antibodies were obtained from Sigma (St. Louis, MO), Southern Biotechnology (Birmingham, AL), or generated locally. CD4-FITC and CD8-PC5 directly conjugated fluorescent antibodies were obtained from Pharmingen (San Diego, CA). CD3-FITC and CD38-PE mAbs were obtained from Beckman Coulter.

Immunohistologic Studies

Immunohistochemical staining was performed on 4 μm FFPE sections using standard protocols, including blocking of endogenous peroxidase activity (0.6% H_2O_2 in absolute methanol, 15 min), microwave citrate antigen retrieval (Biogenex, San Ramon, CA), and diluted goat or horse serum and/or avidin-biotin blocking (Vector Laboratories, Burlingame, CA). The slides were then sequentially incubated at 37°C with primary

6

antibody, biotinylated secondary antibody, and avidin-biotin horseradish peroxidase complexes (VectaStainABC, Vector Laboratories), with intervening PBS washes. Bound antibody was detected with 3, 3'-diaminobenzidine plus H_2O_2. Double immunostains also used ABC-alkaline phosphatase and Vector Red phosphatase substrate (Vector Laboratories). Frozen sections were stained as above after acetone fixation, with omission of deparaffinization, antigen retrieval, and blocking steps. For multicolor immunofluorescence staining, frozen sections were first reacted with cytokeratin mAbs in immunoperoxidase assays to localize the TES, then further incubated with fluorophore-conjugated antibodies for 30 min at room temperature, washed, and examined using an Olympus AX70 microscope equipped for multi-color fluorescence and computerized image analysis.

The percentage of thymus area consisting of perivascular space was determined by microscopic examination of hematoxylin and eosin-stained (H&E) and cytokeratin-immunostained sections, using a Zeiss video microscope with grid overlay. Nonlymphoid components of the PVS can also be stained directly with mAb TE7 (11), however, this mAb works only on frozen sections (data not shown). PVS percentages were obtained for at least 6 representative 10X (1.9 mm^2) fields, then averaged to obtain the mean % PVS. The correlation between % PVS obtained using cytokeratin immunostained vs. H&E sections was 0.97.

For quantitation of cell types present in TES and PVS regions, immunostained sections were classified according to the following criteria, using a Zeiss video microscope with grid overlay: 0 = rare to absent positive cells; 1+ = <5% positive cells; 2+ = 5 - 30% positive cells; 3+ = 31 - 80% positive cells; 4+ = >80% positive cells.

Flow Cytometric Studies

Lymphocytes obtained from pediatric and adult thymus were reacted with combinations of directly conjugated fluorescent antibodies for 30 minutes at 4°C, washed with PBS + 1% bovine serum albumin, fixed with 0.4% paraformaldehyde, and analyzed on a FacStar Plus flow cytometer at the Duke University Center for Aids Research Flow Cytometry Facility.

Ligation-Mediated Polymerase Chain Reaction (LM-PCR) Assay

Genomic DNA was isolated from thymocytes as previously described, taking care not to induce random DNA cleavage during the isolation procedure (14, 15). DNA was resuspended in 10 mM Tris, 1mM EDTA and stored at 4°C until assayed.

Ligation Mediated PCR (LM-PCR) to detect double stranded DNA breaks was modified from previously described protocols (14) and optimized for use with human DNA. Breaks occurring 5' or 3' to the T cell receptor beta chain (TCRB) Dβ2.1 locus were analyzed to achieve a maximal 50% detection of V-DJ and D-J breaks occurring at this one of the two human Dβ loci. A double stranded (ds) asymmetrical linker was generated as described (14). Genomic DNA (1-2 μg) was ligated to 20 pmoles of asymmetrical linker for 12-16 hours at 16°C. The reaction was stopped by addition of one volume 10 mM Tris, 50 mM KCl, 0.1% Triton X-100 and heating at 95°C for 15 minutes. Linker-ligated DNA was stored at –20°C.

Serial 8-fold dilutions of linker-ligated human thymus DNA were made into mock linker-ligated mouse DNA to keep the total amount of DNA constant for each sample.

Double stranded DNA breaks were then detected by nested PCR using a linker-specific

primer and primers which flank the Dβ2.1 locus:

linker 2 primer 5'(CCGGGAGATCTGAATTCCAC)3',

outer forward primer 5'(GGAGTTCAGACATCGTTCAG)3',

outer reverse primer 5'(CCACCAATTTGCAGAGGAGA)3',

inner forward primer 5'(CTGGATTGTTTGTCCTCCTG)3',

and inner reverse primer 5'(GGGACAACACAGTGGATTTG)3'. Nested PCR (60 s, 94°C;

30 s, 94°C,; 30 s, 62°C; 45 s,72°C with a final 8 minute extension step at 72°C) was

performed in 37 µl reactions (Gibco) in hot start PCR tubes or by heated lid PCR. First

round PCR reactions contained 20 µM each of linker 2 primer and forward outer or reverse

outer primer along with 219 ng starting DNA. First round PCR reactions were carried out

for 15 cycles. 2 µl of each reaction were carried into second round PCR containing 20 µM

each linker 2 and forward inner or reverse inner primer for 30 cycles. Template control PCR

reactions using forward outer and reverse outer primers only were carried out for 35 cycles.

PCR products were analyzed on a 2% agarose gel, blotted according to standard

procedures, then detected with a ^{32}P labeled cDNA probe corresponding to bp 277-943 of

the TCRB locus (16).

Lymphocyte Binding Assay

The adherence of human PBMC to high endothelial venules (HEV) in the thymic PVS was

performed as described (17, 18). 12 µm frozen thymus or control tissue sections were

overlaid with 200 µl of PBMC at 15 x 10^{6} cells/ml and incubated at 4°C with rotation (64

rpm) for 30 minutes. The cell suspension was gently decanted and the slides were fixed in

2.4% gluteraldehyde in PBS overnight at 4°C. Slides were then washed twice with PBS, counterstained with hematoxylin, and mounted with glycerol gelatin (Sigma). The number of PBMC adherent to each HEV was determined by direct microscopic visualization of coded slides by a blinded observer. The total number and location of HEV in each section was confirmed by MECA-79 immunostaining of an adjacent tissue section.

RNase Protection Assays

Total RNA was isolated from approximately 100 mg of tissue by homogenization with an Omni International (Marietta, GA) tissue disrupter fitted with disposable 7 mm tips in 1 ml of Trizol (Life Technologies), then extraction per the manufacturer's protocol. Total RNA concentration was determined by absorbance at 260 nm. Steady-state levels of specific cytokine mRNAs in tissues were determined using the multi-probe RiboQuant RNase Protection System (Pharmingen, San Diego, CA). Ten μg RNA per tissue were hybridized overnight with ^{32}P-labeled riboprobe sets (Pharmingen) then processed as described in the manufacturer's instructions. Protected RNA transcripts were separated on a 5% denaturing polyacrylamide gel (National Diagnostics, Atlanta, GA). Cytokine mRNA bands were quantified by phosphorimager (Molecular Dynamics, Sunnyville, CA) analysis and reported as % of GAPDH signal.

Results

Thymic PVS volume increases with age in normal subjects and in myasthenia gravis patients. Although grossly detectable thymic atrophy may not occur until puberty, analysis of thymic PVS in normal thymus tissues ranging from age 0 to 78 (Table 1) clearly

demonstrates that a statistically significant increase in the PVS has occurred by 2 – 10

years of age (age quintile 2, p<0.01 relative to age quintile 1, 0 –1 yr) (Figure 1A). The %

PVS increases progressively with age in normal individuals (Figure 1A), in agreement with

previous studies by Steinmann (2). Increase in PVS volume is accompanied by

accumulation of lymphocytes within the PVS (Figure 1C – H), particularly in quintiles 2-4.

The contribution of the TES and the PVS to the overall composition of MG

thymus during aging was determined and compared to normal thymus. The % PVS is

increased in MG relative to age-matched normal thymuses (quintile 2, p<0.07; quintile 3,

p<0.08; quintile 4, p<0.0006; quintile5, p<0.018) (Figure 1B). A portion of this increase

is due to follicular hyperplasia present in a subset of MG thymus tissue (Table 1).

Cytokeratin staining (Figure 1H) clearly demonstrates that the primary and secondary

follicles present in MG thymus with follicular hyperplasia occur in the PVS, not in the

TES, similar to what is observed in normal aging thymus (5). Thus, the thymic follicular

hyperplasia seen in the PVS of MG thymus is an exaggerated state of the perivascular

infiltration with lymphocytes that normally occurs in aging thymus.

The adipocyte and lymphocyte content of the PVS similarly changes with age.

Adipocytes are rare in quintile 1, and increase progressively in quintiles 2 – 5, as shown in

Figure 1. The lymphocyte content of the PVS increases rapidly in quintiles 2 and 3, such

that a significant fraction of PVS area in these age ranges contains lymphocytes (Figure

1D, &E), as previously reported by Steinmann (2). The lymphocyte content of the PVS

begins to decrease in quintile 4, with corresponding increase in the fraction of PVS

composed of adipose tissue in quintiles 4 and 5 relative to earlier quintiles (Figure 1F &

G). The PVS of most tissues in quintile 5 contains predominately adipocytes, with few

lymphocytes (Figure 1G).

Immunohistologic identification of cells undergoing thymopoiesis in the TES. The TES in

both normal and MG thymus decreases with age as PVS increases (Figure 1A & B). To

study changes in thymopoiesis with age, we have determined the phenotype of

lymphocytes present in the TES of normal and MG thymus tissues. CD1a is expressed on

immature $CD4^+$ $CD8^+$ (double positive) cortical thymocytes that have successfully

completed rearrangement of the TCR beta chain (TCRB) gene locus (19), but is not

expressed on medullary thymocytes or mature T cells (20). We found that CD1a

immunoreactivity in infant thymus (age 0-1 yr) was limited to thymocytes within the

thymic cortex (not shown). Some dendritic cells located in the thymic medulla also reacted

with CD1a mAb, however these cells were clearly distinguished from immature

thymocytes by their location, larger size, and multiple dendritic processes. Rare $CD1a^+$

cells with dendritic cell morphology were also present in the PVS. The majority of the

$CD1a^+$ cortical thymocytes also reacted with mib-1 mAb specific for the Ki-67 nuclear

proliferation antigen, with less frequent $mib-1^+$ cells present in the thymic medulla and in

the PVS (not shown). $CD1a^+$ $mib-1^+$ cortical thymocytes also reacted strongly with

antibodies specific for CD3, CD4, CD8, CD38, and CD45RO (not shown), as expected

for immature thymocytes (20, 21). Only rare isolated lymphocytes within the TES were

reactive with TIA-1 mAb, specific for granules present in activated CTL. Cytokeratin

staining revealed a loose network of TE cells within the cortex in association with large

numbers of $CD1a^+$, $mib-1^+$ thymocytes, with a somewhat denser pattern of TE cells in the

medulla (not shown). The majority of TE cells in both cortex and medulla were surrounded by multiple thymocytes. Taken together, these studies suggest that thymus tissues active in the process of thymopoiesis can be identified immunohistologically in FFPE tissues by the presence of immature CD1a$^+$mib-1$^+$ thymocytes in a loose network of TE cells that allows thymocyte/TE interactions.

116 of the 118 normal and MG thymus tissues examined contained at least some regions meeting our immunohistologic criteria for thymopoiesis. However, the absolute numbers of immature CD1a$^+$ mib-1$^+$ thymocytes undergoing thymopoiesis decreased progressively as the %TES decreased with age and in MG. Thymocytes derived from a 78 yr old male thymus shown by immunohistochemistry to contain CD1a$^+$mib-1$^+$thymocytes have an immature phenotype. These thymocytes are CD4+ and CD8+, express CD45RO and CD38, and are negative for CD95, CD62L and CD45RA (Figure 2). This thymus was highly atrophic with few PVS lymphocytes present. Although the absolute numbers of immature thymocytes were greatly decreased, the relative proportions were similar to pediatric thymus.

LM-PCR detects ongoing TCR gene rearrangement in pediatric and adult human thymocytes. To provide molecular confirmation of thymopoiesis, we used a ligation mediated PCR assay (LM-PCR) (22, 14) to identify double stranded DNA breaks indicative of D-J or V-DJ T-cell receptor gene rearrangement in thymocytes derived from pediatric and adult thymus tissues. This assay detects dsDNA breaks transiently generated at recombination signal sequences by the VDJ recombinase complex during the process of

TCR gene rearrangement (Figure 3A). The presence of LM-PCR signals in a given tissue is thus indicative of ongoing thymopoiesis.

LM-PCR analysis detected DNA breaks associated with both D-J and V-DJ rearrangement of the TCR beta chain gene in 14 of 14 pediatric thymocyte samples tested (2 representative samples shown in Figure 3B, lanes 1,3,9,11). This assay is specific for ongoing human TCRB gene rearrangement, as no LM-PCR signals are detected in DNA from human spleen or tonsil, mouse thymocytes (data not shown), bacteria (Figure 3B, lanes 5,6,13,14) or mock linker ligated thymocytes (Figure 3B, lanes 2,4,10,12).

LM-PCR was used to determine whether the phenotypically immature thymocytes present in older adult thymuses were undergoing thymopoiesis. LM-PCR analysis detected dsDNA breaks corresponding to both D-J and V-DJ TCR gene rearrangement in most thymocyte DNA samples derived from normal adult and MG thymus tissues showing immunohistologic evidence of thymopoiesis (Figure 3C). LM-PCR signals corresponding to D-J TCR gene rearrangement were detected in 8 of 8 adult thymus tissues tested, with V-DJ signals detected in 5 of 8 samples.

Eosinophils are prominent in the PVS of pediatric thymus. The PVS of infant (quintile 1, 0 – 1 yr) thymus contains few lymphocytes. The majority of the cells present in the PVS of infants are spindle-shaped, consistent with fibroblasts or pre-adipocytes. However, large clusters of eosinophils are also frequently found in the PVS of infant thymus (Figure 4A). While many of these eosinophils have the bilobed nucleus characteristic of mature eosinophils, cells containing similar eosinophilic granules and large single-lobed or indented nuclei with chromatin patterns consistent with the eosinophilic myelocyte and

eosinophilic metamyelocyte stages of eosinophil differentiation are also present. Clusters of eosinophils are smaller and less abundant in older children (quintile 2, 2 – 10 yrs). Eosinophils are rare to non-detectable in older thymus tissues from age quintiles 3 – 5 (≥11 yrs).

The eosinophils present within the PVS of pediatric thymus could have differentiated there *in situ* or could have developed inside the TES or outside the thymus, then migrated into the PVS. To investigate the ability of the thymus to support the differentiation of eosinophils, we analyzed thymic IL-5 mRNA production as a function of age. In humans, IL-5 is highly specific for stimulating the production, activation, and survival of eosinophils (23). In mice, the expression of IL-5 is sufficient to induce the full pathway of eosinophil differentiation (24). We therefore analyzed the expression of IL-5 in 44 normal human thymus tissues by RNase protection assay. We found that IL-5 was readily detectable in most normal thymus tissues from patients aged ≤2 years (IL-5 =1.13 ± 0.28 % of GAPDH signal, range 0 – 3.28, n = 14). IL-5 mRNA was undetectable in thymus derived from patients ≥ 3 years of age (n = 30). The level of IL-5 mRNA correlates with the observed incidence of eosinophilia within the thymic PVS in patients ≤ 3 yrs of age. In particular, thymus tissues with high IL-5 content had moderate to large clusters of eosinophils present in the PVS (Figure 4A). Conversely, thymic tissues with undetectable IL-5 mRNA levels did not demonstrate eosinophilia of the thymic PVS. Taken together, with the observation that some of the eosinophils present in the PVS exhibit nuclear morphologies characteristic of immature eosinophils, these data suggest that the eosinophils present in the thymic PVS of infants could differentiate in the PVS in response to thymic IL-5 production.

PVS lymphocytes have a phenotype consistent with peripheral lymphocytes. As described

above, T lymphocytes present within the PVS are not CD1a$^+$ and mib-1$^+$ and are thus most

likely mature T lymphocytes. Mature T lymphocytes present in the PVS may be newly

generated mature virgin T cells emigrating from the thymus or T cells recirculating from

the periphery. No phenotypic markers currently exist to specifically detect recent thymic

emigrants in humans. Therefore, we determined the immunoreactivity of PVS lymphocytes

with a panel of antibodies directed at lymphocyte differentiation and activation markers,

using single, double and triple immunohistochemical and immunofluorescence assays to

localize both the PVS (by lack of cytokeratin reactivity, Figure 5A,B) and to identify

appropriate markers on lymphocytes. Results are summarized in Table 2.

When large numbers of lymphocytes are present in the PVS of normal thymus

(usually in age quintiles 3 and 4), the infiltrate consists of both T and B cells (Figure 5C,

D). T cells in the PVS are CD1a$^-$ and most are also mib-1$^-$ (Figure 5E, F). Triple

immunostains, combining a cytokeratin immunoperoxidase stain to localize the TES with

CD4-FITC and CD8-PC5 fluorescent antibodies, demonstrated that PVS T cells are single

positive, expressing either CD4 or CD8, but not both (not shown; see also Figure 5G).

Most PVS T cells express the CD45RO cell surface antigen (Figure 5H) rather than the

CD45RA antigen typically expressed on peripheral virgin T cells (not shown). Although

large numbers of CD45RA$^+$ lymphocytes are present in both the thymic medulla and in the

PVS, the majority of these cells are B cells (Figure 4B). The cell types present in the PVS

of 50 normal adult and 31 age-matched MG thymus tissues are similar, with further

expansion of the PVS in MG thymus with follicular hyperplasia by infiltrates of primarily

B lymphocytes, often with prominent germinal centers. (Figure 1H).

We observed that a subset of the CD8^{+} T cells present in the PVS also express the

TIA-1 antigen characteristic of activated CTL (Figure 4C), indicating that these cells are

not recent thymic emigrants, but are mature CTL from the periphery (25). We also found

differences in CD38 expression between T cells in the TES and the PVS. Although

cortical and medullary thymocytes express relatively high reactivity with CD38 mAb (21)(

Figure 2E), most T cells present in the PVS do not have high reactivity with CD38.

However, germinal center B cells are moderately to strongly reactive with CD38 mAbs

(Table 2). Using cytokeratin immunoperoxidase staining to localize the TES, combined

with CD3-FITC and CD38-PE mAbs, we confirmed that virtually all CD3^{+} T cells within

the TES are also strongly positive for CD38 mAb (data not shown). Conversely, in the

PVS, the majority of CD3^{+} cells are not strongly reactive with CD38 mAb. Less that 5%

of PVS CD3^{+} cells reacted strongly with CD38 mAb, and these cells were frequently

located within or adjacent to B cell follicles with germinal centers, consistent with an

activated T cell phenotype. The relative lack of CD38 immunostaining of most PVS T

cells is also consistent with a peripheral origin for most PVS lymphocytes, as most

peripheral blood lymphocytes are also CD38^{-} (21).

PBMC bind to MECA-79 [+] *HEV in the PVS of adult normal and MG thymus.* We

observed that high endothelial venules (HEV) could frequently be identified in normal

thymus PVS when large numbers of lymphocytes were present in the PVS. Similarly,

17

thymus from adult patients with MG that had large PVS lymphoid infiltrates also contained HEV within the PVS. Peripheral lymph node HEV have previously been shown to be immunoreactive with MECA79 mAb, which recognizes a ligand for L-selectin (13). We found that the HEV present in the PVS of adult normal and MG thymus react strongly with MECA79 mAb (Figure 5I) similar to HEV in lymph node that have been shown to support lymphocyte recirculation via a MECA-79/L-selectin dependent mechanism (26). Thymic PVS HEV did not react with mAb MECA-367 (not shown), specific for a mucosal addressin previously shown to direct migration of lymphocytes to Peyer's patches and mesenteric lymph node (12, 27, 28).

To determine whether the thymic PVS HEV can potentially support the emigration of peripheral lymphocytes, we performed *in vitro* assays of PBMC binding to tissue sections, as previously described (17, 18). We found that PBMC bound specifically to thymic PVS HEV, with 14 ± 3 lymphocytes (mean $\pm$ SD) bound per HEV in the 4 thymus tissues tested . These studies demonstrate that PBMC bind well to the MECA-79^{+} thymic HEV, which can thus potentially direct the migration of peripheral lymphocytes into the thymic PVS. Additional studies will be needed to determine the precise mechanisms for lymphocyte emigration into the PVS.

Discussion

In this paper, we have extensively characterized the thymic PVS of adults, and provide data suggesting the peripheral origin of PVS lymphocytes. Our identification of

MECA-79[+] HEV that are capable of binding PBMC suggests a mechanism for egress of peripheral lymphocytes into the PVS.

Our data on the relative proportions of the TES and PVS in normal thymus are consistent with those of Steinmann (2), who used silver staining to identify PVS containing reticular fibers associated with extracellular matrix deposition. The PVS can also be identified by immunostains for fibronectin and laminin (3, 29) and by mAb TE7 (11). In this study we delineated the PVS from the TES (cortex and medulla) using reactivity of the epithelial component of the TES with cytokeratin mAbs as a marker. We have determined the epithelial content of aging thymus, including the development of immunohistologic assays to evaluate the extent of ongoing thymopoiesis in archival formalin-fixed paraffin embedded (FFPE) thymus tissues.

We also report a definitive molecular assay for ongoing thymopoiesis in the human thymus using the LM-PCR assay to detect double stranded DNA breaks that occur specifically during TCR gene rearrangement. Previous studies have used LM-PCR to investigate VDJ recombination in mouse thymocytes (14, 22). Recent studies have measured the levels of T-cell receptor excised circles (TRECs) in blood lymphocytes to estimate levels of thymopoiesis (30, 31,32). However, since TRECs are long lived in peripheral T-cells, and are lost only by dilution during cellular proliferation, a direct correlation between TREC levels and ongoing thymopoiesis cannot be made with this assay. The LM-PCR assay provides a snapshot of ongoing TCR gene rearrangement at the time of tissue harvest, and this provides a definitive measure of thymopoiesis in cases where fresh thymus tissue is available.

19

Our studies of lymphocytes in the TES demonstrated that the presence of mature

CTL, as indicated by expression of the TIA-1 granule antigen, is rare within the TES.

These results fail to directly support the hypothesis of Hartwig and Steinmann (6) that

such cells are responsible for induction of atrophy in aging thymus. We did find that TIA-

1^+ CTL are often present in the PVS of both normal and MG adult thymus tissues (Figure

4C). Since cells in the PVS are separated from the TES by a basement membrane (3), the

anatomic localization of thymic CTL make it less likely that these CTL induce atrophy of

the TES through direct effects on thymic epithelial cells. However, CTL in the PVS could

secrete cytokines that may have direct or indirect effects on the process of thymic atrophy.

We also studied the PVS of MG human thymus tissues in parallel with normal

thymus tissue. As previously reported, we found that histologic changes that occur in

normal human thymus with aging also occur in MG thymus. The follicular hyperplasia

observed in some of the MG thymus tissues is histologically similar, although

quantitatively exaggerated, to changes occurring in normal thymus during aging.

Therefore, both normal and MG thymus can be used to illustrate the changes that occur in

the PVS and TES of the human thymus with aging.

We report several other novel observations. First, although eosinophils have

previously been identified within thymus tissue of infants (33, 34), their location within the

PVS as well as their decreased prevalence with age has never been described. Our data

showed that thymus from children ≤ 2 years old potentially contains sufficient IL-5 to

support eosinophil differentiation, consistent with the hypothesis that eosinophils

differentiate *in situ* within the PVS of pediatric thymus early in life. However, as IL-5 has

been shown to also be chemotactic for eosinophils (35, 36), increased eosinophil migration into the PVS of IL-5-expressing pediatric thymus tissues cannot be ruled out.

Although several studies have suggested that lymphocytes present within the PVS may be of peripheral origin (see below), our study is the first to demonstrate that these PVS lymphocytes are immunophenotypically consistent with peripheral mature cells. Although many surface markers expressed on PVS lymphocytes are also expressed on lymphocytes present in the thymic medulla, the presence of large numbers of $CD1a^-$ $CD45RO^+$ $CD38^{-/low}$ T cells combined with the presence of $TIA-1^+$ activated CTL within the PVS, demonstrated that at least some PVS T cells are not new virgin T cells exiting from the thymic medulla and thus are likely to have migrated from the periphery. The presence of B cells located clearly within in the thymic medulla (Figure 4B) raises the question of whether these cells arise in the medulla, in contrast to PVS B cells that may come from the periphery. The contribution of the thymus to the process of B cell development has been understudied, and the potential contributions of thymic B cells to the peripheral immune B cell repertoire remain unclear.

The question of whether T-cells in the thymic PVS originate within the thymus or migrate from the periphery has been previously addressed in animal models. Savino et al (29) described the existence of giant thymic PVS in the non-obese diabetic (NOD) mouse. Cells within the PVS of these animals were resistant to sublethal X-irradiation and hydrocortisone treatment, and were concluded to be mature lymphocytes, consistent with our more extensive phenotypic characterization of PVS cells in human thymus.

Finally, the identification and localization of HEV within the PVS of human thymus is important. The existence of HEV within the thymus has previously been

reported in preleukemic mice (37), although those authors did not recognize the existence of the PVS and described these HEV to occur within thymic medulla. "Occasional, predominately medullary MECA-79+ HEV" were previously reported in postnatal human thymus (38), however the significance was not discussed and anatomic localization was similarly imprecise. The expression of MECA-79, a ligand for L-selectin, on the HEV in the PVS suggests a mechanism by which peripheral lymphocytes could access the thymic PVS, similar to mechanisms described in peripheral lymph nodes and sites of inflammation (38). Our studies using *in vitro* lymphocyte binding assays demonstrate that peripheral blood lymphocytes can bind to thymic HEV and thus potentially migrate into the thymic PVS. The function of these PVS lymphocytes in relation to the process of thymic involution has not been established, although temporally, the largest infiltrates are seen in the age ranges where more rapid involution occurs. The mechanisms regulating HEV development in the PVS are still unknown.

Taken together, our studies suggest that the thymic PVS is a compartment of the peripheral immune system that is not directly involved in thymopoiesis. Understanding the relationships between the trafficking of peripheral lymphocytes to thymic PVS should lead to insights into mechanisms of thymic atrophy and control of postnatal thymic function.

Table 1

Characteristics of Thymus Tissues Studied*

Age Quintile*

Diagnosis	1	2	3	4	5
Cardiothoracic Surgery	18 (10/7/1)#	17 (10/7)	5 (2/3)	8 (3/5)	7 (5/2)
Mediastinal Mass	0	1 (0/1)	0	2 (1/1)	0
Thyroid/ Parathyroid	0	1 (0/1)	5 (2/3)	8 (2/6)	12 (0/12)
Trauma	0	0	0	3 (3/0)	0
Normal Tissues	18 (10/7/1)	19 (10/9)	10 (4/6)	21 (9/12)	19 (5/14)
Total Normal Tissues 87 (38/48/1)					
MG	0	2 (0/2)	8 (2/6)	13 (5/8)	8 (6/2)
% with follicular hyperplasia		50%	63%	31%	32%
Total MG tissues	31 (13/18)				

*Data are expressed as total number of tissues (males/females) in each diagnosis category.

Age quintiles are defined as follows: 1 = 0 – 1 yr; 2 = 2 – 10 yr; 3 = 11 – 25 yr; 4 = 26 – 49 yr; 5 = ≥ 50 yr.

In age quintile 1, the gender of one thymus donor was not recorded.

Table 2

Immunoreactivity of Lymphocytes Present in the Thymic Compartments

Antibody	Cortex	Medulla	Perivascular Space
CD3	++++	+++	+++
CD1a	++++	- *	- *
mib-1	+++	+	++
CD20	+	+++	+++
CD45RA	+	+++	++
CD45RO	++++	+++	+++
TIA-1	- **	- **	+
CD4	++++	++	++
CD8	++++	+++	++
CD4 + CD8	++++	-	-
CD38	++++	+++	++***
CD3 + CD38	++++	+++	+

* Positive on cells with dendritic morphology only.

** Positive only on rare cells.

*** Positive on B and T cells within germinal centers.

Scoring system as described in Materials and Methods. Data are representative of 6 to 70 tissues examined for single stains, and 3 to 5 tissues for double stains

Figure 1: Thymic PVS increases with age in normal individuals and patients with myasthenia gravis. The percent thymic PVS determined from H&E-stained sections is shown as a function of age quintile. **Panel A**: Data for normal individuals are expressed as mean ± standard deviation for the indicated number of cases. Quintile 1 (0 – 1 yr), 7 ± 2%, n = 18; Quintile 2 (2 – 10 yr), 12 ± 7%, n = 19; Quintile 3 (11 – 25 yr), 37± 19%, n = 10; Quintile 4 (26 – 49 yr), 55 ± 18%, n = 21; Quintile 5 ($\geq$50 yr), 82 ± 16%, n = 19. **B.** Data for patients with myasthenia gravis are expressed as mean ± standard deviation for the indicated number of cases. Quintile 2, 23 ± 13%, n = 2; Quintile 3, 61 ± 34%, n = 8; Quintile 4, 83 ± 14%, n = 13; Quintile 5, 96 ± 2%, n = 8. **Panel C-H**, Cytokeratin immunoperoxidase staining (brown color) outlines TES, with an H&E counterstain. Letters denote representative regions of thymic cortex (C), medulla (M), and PVS (P). **Panel C**, Quintile 1; **Panel D**, Quintile 2; **Panel E**, Quintile 3; **Panel F**, Quintile 4; **Panel G**, Quintile 5. **Panel H** shows thymus with follicular hyperplasia from a 20 year old female with MG. Cytokeratin/H&E staining shows that primary and secondary follicles are located outside the cytokeratin network, within the PVS (original magnification, x25).

Figure 2. Phenotypically immature thymocytes are present in adult thymus tissues meeting immunohistologic criteria for thymopoiesis. Lymphocytes from a 78 year old male thymus were analyzed by flow cytometry using combinations of fluorescently labeled mAbs. The majority of lymphocytes present were CD3$^+$ (**Panel A**), with 82% CD4$^+$, CD8$^+$ double positive (**Panel B**). Of the CD4^{hi} cells, greater than 90% were CD45RO$^+$ (**Panel D**), 97% were CD38$^+$(**Panel E**), and 97% were CD45RA$^-$ (**Panel F**) consistent with an

immature phenotype. Similar results were seen with gating on CD8+ lymphocytes. Less than 3% of cells were reactive with CD19 and CD20 mAbs (**Panel C**) and are thus identified as B lymphocytes. Very few mature T-cells were present in this sample, consistent with the observed lack of lymphocytes infiltrating the PVS on immunohistochemical sections. Although the majority of cells present in this thymus were immature thymocytes, the absolute numbers of thymocytes obtained for analysis were less than 1% of those obtained per gram of tissue from pediatric thymus.

Figure 3. LM-PCR detects ongoing TCR gene rearrangement in pediatric and adult thymocytes. **A**: Ligation-mediated PCR detects free signal ends generated by dsDNA breaks 3' and 5' of the Dβ2.1 TCR gene segment, corresponding to D-J and V-DJ rearrangements, respectively. **Panel B** demonstrates specific LM-PCR products obtained from thymocytes from 2 normal individuals < 6 months old, indicating ongoing V-DJ (lanes 1 and 3; 409 bp) and D-J (lanes 9 and 11; 492 bp) rearrangement. Controls with non-linker ligated DNA amplified with primers 3 and 5 (lane 17) or 2 and 4 (lane 18) demonstrate the appropriate sized germline bands (868 and 956 bp, respectively). Lanes using mock ligated DNA (lanes 2, 4, 10, 12), DNA lacking the TCR loci (bacterial DNA ± linker ligation, lanes 5, 6, 13, 14), linker alone (lanes 7, 15), and PCR blanks (lanes 8, 16) are negative. The higher molecular weight bands seen in lanes 1 and 11 most likely represent dsDNA breaks corresponding to additional (nonproductive) rearrangements in cells with a rearranged Dβ2.1 locus, however this remains to be formally demonstrated using probes and primers specific for sequences unique to these downstream regions. **Panel C** shows LM-PCR signals generated from thymocytes obtained from a 24 year old

male. 8-fold dilutions of DNA (decreasing concentration, left to right) were linker-ligated and subjected to LM-PCR as described. Signals corresponding to both D-J and V-DJ rearrangements were detected in 5 of 8 samples (donor age/gender: 24M, 29F, 27F, 41F, 42F) . Only D-J signals were detected in 3 samples (donor age/gender: 28F, 34F, 46M). All tissues tested had immunohistologic evidence for thymopoiesis, with at least small foci of $CD1a^+$ mib-1^+ lymphocytes within a loose network of thymic epithelial cells. Template control reactions using primers 2 & 4 amplified the appropriate sized germline band.

Figure 4: Phenotypes of cells present in the thymic PVS. Panel A: H&E plus cytokeratin immunoperoxidase staining (brown) demonstrates that eosinophils are present outside the TE network and thus within the PVS in thymus tissues expressing IL-5 mRNA. The majority of cells shown in this field are eosinophils, with both mature and immature morphologies represented. Arrows denote representative eosinophils. **Panel B**: Cytokeratin (brown) and CD20 (red) doublestain shows that $CD20^+$ cells are present within both the thymic medulla (M) and the PVS (*), but are rare within the cortex (C). **Panel C**: Cytokeratin (brown) and TIA-1 (red) doublestain identifies TIA-1^+ cells within the PVS.

Figure 5: Phenotypes of cells present in the thymic PVS. Thymus from a 42 year old female with MG is shown to allow examination of relatively large areas of PVS within a single field. TES active in thymopoiesis is highlighted using a C to indicate active cortex, with an arrow pointing to the medulla. The cytokeratin stain (**Panel B**) also demonstrates inactive TES (arrowheads in panels A&B) surrounded by PVS (P). The following

immunoperoxidase stains demonstrate phenotypes of cells present in both TES and PVS: **Panel C**: CD3, T-cells; **Panel D**: CD20, B-cells; **Panel E**: CD1a, immature thymocytes; **Panel F**: mib-1, proliferating cells Note the positive reaction of both CD1a and mib-1 mAbs (brown) with thymocytes in cortex (C) but not in medulla (arrow).; **Panel G**: CD8, immature thymocytes and mature cytotoxic T-cells; **Panel H**: CD45RO, immature thymocytes and mature memory T-cells; **Panel I** :MECA-79 immunostaining highlights high endothelial venules in the thymic PVS (P). Inset depicts a MECA-79 + high endothelial venule at higher magnification.

References

1. Steinmann , G.G., Klaus, B. 1985. The involution of the ageing human thymic epithelium is independent of puberty. A morphometric study. *Scand. J. Immunol.* 22: 563-575.

2. Steinmann, G.G. 1986. Changes in the human thymus during aging. *Curr. Top. Pathol.* 75:43-88.

3. Bofill, M., Janossy, G., Willcox, N., Chilosi, M., Trejdosiewicz, L.K., Newsome-Davis, J. 1985. Microenvironments in the normal thymus and the thymus in myasthenia gravis. *Am. J. Pathol.*119: 462-473.

4. Kato, S., Schoefl, G.I. 1989. Microvasculature of normal and involuted mouse thymus: light and electro microscopic study. *Acta. Anat.* 135: 1-11.

5. Tamaoki, N., Habu, S., Kameya, T. 1971. Thymic lymphoid follicles in autoimmune disease: Histologic, histochemical, and electron microscopic studies. *Keio Med. J.* 20:57-68.

6. Hartwig, M., Steinmann G. 1994. On a casual mechanism of chronic thymic involution in man. *Mech. Ageing Develop.* 75: 151-156.

7. Krenacs, L. Tiszolvicz, L., Krenacs, T., Boumsell, L. 1993. Immunohistochemical detection of CD1a antigen in formalin-fixed and paraffin-embedded tissue sections with monoclonal antibody O10. *J. Pathol.* 171:99-104.

8. Mason, D.Y., Cordell, J., Brown, M., Pallesen, G., Ralfkiaer, E., et al. 1989. Detection of T cells in paraffin wax embedded tissue using antibodies against a peptide sequence from CD3 antigen. *J. Clin. Pathol.* 42: 1194-1200.

9. Key, G., Becker, M., Baron, B., Duchrow, M., Schluter, C. 1993. New Ki-67-equivalent murine monoclonal antibodies (MIB 1-3), generated against bacterially expressed parts of the Ki-67 DNA containing three 62 base pair repetitive elements encoding the Ki-67 epitope. *Lab Investig.* 68:629-636.

10. Anderson, P., Nagler-Anderson, C., O-Brien, C., Levine ,H., Watkins, S., Slayter, H.S., et al. 1990. A monoclonal antibody reactive with a 15-kDa cytoplasmic granule-associated protein defines a subpopulation of CD8+ T lymphocytes. *J. Immunol.* 144:574-582.

11. Haynes, B.F., Scearce, R.M., Lobach, D.F., Hensley, L.L. 1984. Phenotypic characterization and ontogeny of mesodermal-derived and endocrine epithelial components of the human thymic microenvironment. *J. Exp. Med.* 159: 1149-1168.

12. Streeter, P.R., Berg, E.L., Rouse, B.N., Bargatze, R.F., Butcher, E.C. 1988. A tissue-specific endothelial cell molecule involved in lymphocyte homing. *Nature.* 331:41-46.

13. Streeter, P.R. Rouse, B.T.N., Butcher, E.C. 1988. Immunohistologic and functional characterization of a vascular addressin involved in lymphocyte homing into peripheral lymph nodes. *J. Cell. Biol.* 107:1853-1862.

14. McMurry, M., Hernandez-Martin, C., Lauzurica, P., Krangel, M.S. 1997. Enhancer control of local accessibility to the VDJ recombinase. *Molec. Cell. Biol.* 17:4553-4561.

15. Ausubel, F.M., Brent, R., Kingston, R.E., Moore, D.D., Seidman, J.G., et al. 1997. *Current Protocols in Molecular Biology*, John Wiley and Sons.

16. Toyonaga, B., Yoshikai, Y., Vadasz, V., Chin, B., Mak, T.W. 1985. Organization and sequences of the diversity, joining, and constant regions of the human T-cell beta chain. *Proc. Natl. Acad. Sci.* USA 82:8624-8628.

17. Stamper, H.B., Woodruff, J.J. 1976. Lymphocyte homing into lymph nodes: in vitro demonstration of the selective affinity of recirculating lymphocytes for high endothelial venules. *J. Exp. Med.* 144:828-833.

18. Steeber, D.A., Green, N.E., Sato, S., Tedder, T.F. 1996. Lymphocyte migration in L-selectin-deficient mice: altered subset migration and aging of the immune system. *J. Immunol.* 157:1096-1106.

19. Rothenberg, E.V. 1992. The development of functionally responsive T cells. *Adv. Immunol.* 51: 85-214.

20. Haynes, B.F., Denning, S.M., Le, P.T., Singer, K.H. 1990. Human intrathymic T cell differentiation. *Seminars in Immunology.* 2:67-77.

21. Malavasi, F., Funaro, A., Roggero, S., Horenstein, A., Calosso, L., Mehta, K. 1994. Human CD38: a glycoprotein in search of a function. *Immunol. Today.* 15: 95-97.

22. Roth, D.B., Zhu, C.,Gellert, M. 1993. Characterization of broken DNA molecules associated with V(D)J recombination. Proc. *Natl. Acad. Sci. USA.* 90:10788-10792.

23. Sanderson, C.J., Karlen, S., Cornelis, S., Plaetinck, G., Tavernier, J., Devos, R. 1998. *Interleukin-5* in *Cytokines.* Mire-Sluis A, Thorpe R, editors. Academic Press : London. 69-80.

24. Dent, L.A., Strath, M., Mellor, A.L., Sanderson, C.J. 1990. Eosinophilia in transgenic mice expressing IL-5. *J. Exp. Med.* 172:1425-1431.

25. Gossman, J., Lohler J., Lehmann-Grube, F. 1991. Entry of antivirally active T lymphocytes into the thymus of virus-infected mice. *J. Immunol.* 146: 293-297.

26. Berg, E.L., Robinson, M.K., Warnock, R.A., Butcher, E.C. 1991. The human peripheral lymph node vascular addressin is a ligand for LECAM-1, the peripheral lymph node homing receptor. *J. Cell Biol.* 114:343-349.

27. Bargatze, R.F., Jutila ,M.A,. Butcher, E.C. 1995. Distinct roles of L-selectin and integrins $\alpha_4\beta_7$ and LFA-1 in lymphocyte homing to Peyer's patch-HEV in situ: The multi-step model confirmed and refined. *Immunity.* 3:99-108.

28. Berlin, C., Berg, E.L., Briskin, M.J., Andrew, D.P., Kilshaw, P.J, et al. 1993. $\alpha_4\beta_7$ integrin mediates lymphocyte binding to mucosal vascular addressin MAdCAM-1. *Cell* 74:185-195.

29. Savino, W., Carnaud, C., Luan, J-J., Bach, J-F., Dardenne, M. 1993. Characterization of the extracellular matrix-containing giant perivascular spaces in the NOD mouse thymus. *Diabetes.* 42:134-140.

30. Douek, D.C., McFarland, R.D., Keiser, P.H., Gage, E.A., Massey, J.M., et al. 1998. Changes in thymic function with age and during treatment of HIV infection. *Nature.* 396: 690-695.
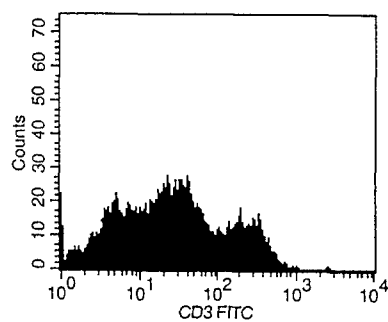
31. Haynes, B.F., Hale, L.P., Weinhold, K.J., Patel, D.D., Liao, H-X, et al. 1999. Analysis of the adult thymus in reconstitution of T lymphocytes in HIV-1 infection. *J. Clin. Invest.* 103: 453-460.

32. Jamieson, B.D., Douek, D.C., Killian, S., Huitin, L.E., Scripture-Adams, D.D, et al. 1999. Generation of functional thymocytes in the human adult. *Immunity.* 10:569-575.

33. Dourov, N. 1982. L'examen microscopique du thymus au cours de la periode perinatale. *Ann. Pathol.* No3: 255-261.

34. Muller, E. 1977. Localization of eosinophils in the thymus by peroxidase reaction. *Histochemistry.* 52: 273-279.

35. Yamaguchi, Y., Hayashi ,Y., Sugama, Y., Miura, Y., Kasahara, T. 1988. Highly purified murine interleukin-5 (IL-5) stimulates eosinophil function and prolongs in vitro survival. *J. Exp. Med.* 167:1737-1742.

36. Wang, J.M., Rambaldi, A., Biondi, A,. Chen, Z.G., Sanderson, C.J., et al. 1989. Recombinant human interleukin 5 is a selective eosinophil chemoattractant. *Eur. J. Immunol.* 19:701-705.

37. Michie, S.A., Streeter, P.R., Butcher, E.C., Rouse, R.V. 1995. L-selectin and $\alpha_4\beta_7$ integrin homing receptor pathways mediate peripheral lymphocyte traffic to AKR mouse hyperplastic thymus. *Am. J. Pathol.* 147:412-421.

38. Michie, S.A., Streeter, P.R., Bolt, P.A., Butcher, E.C., Picker, L.J. 1993. The human peripheral lymph node vascular addressin: an inducible endothelial antigen involved in lymphocyte homing. *Am. J. Pathol.* 143:1688-1698.
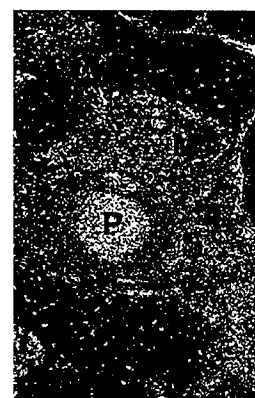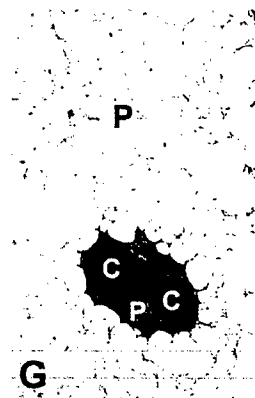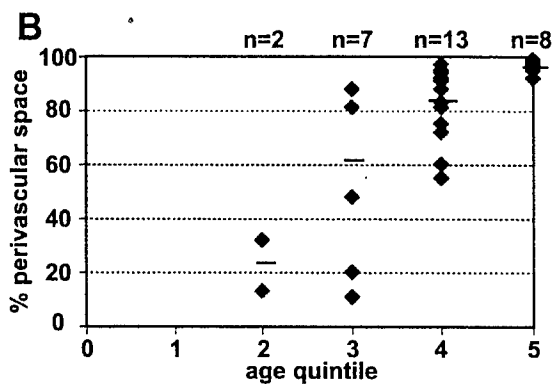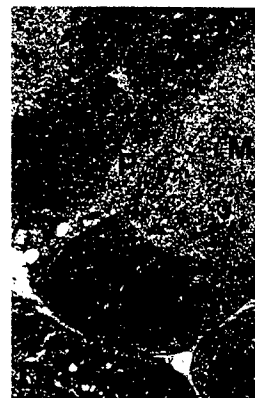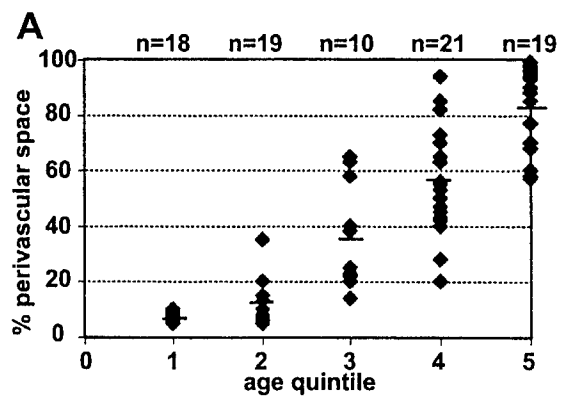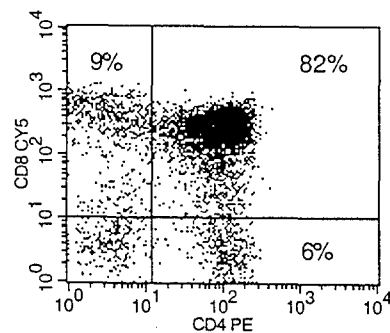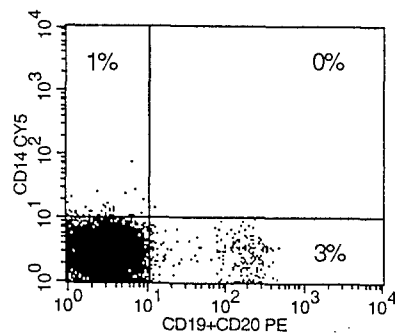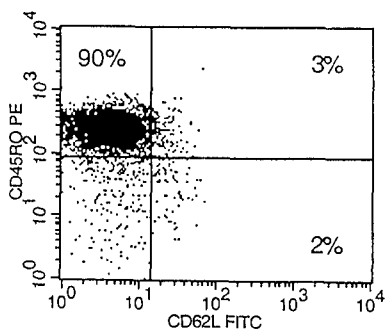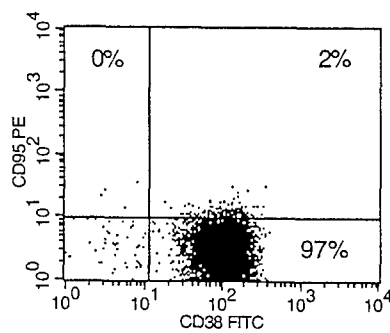
Flores et al
Figure 1

A. Lymphocytes — histogram, Counts vs CD3 FITC

B. Lymphocytes — CD8 CY5 vs CD4 PE; 9%, 82%, 6%

C. Lymphocytes — CD14 CY5 vs CD19+CD20 PE; 1%, 0%, 3%

D. CD4+ Lymphocytes — CD45RO PE vs CD62L FITC; 90%, 3%, 2%

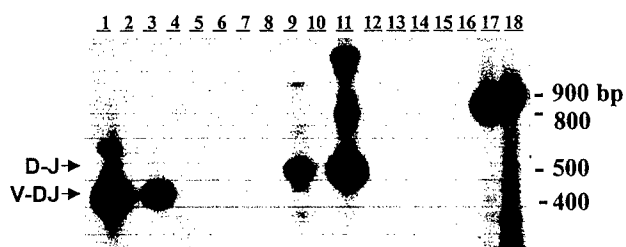**E. CD4+ Lymphocytes** — CD95 PE vs CD38 FITC; 0%, 2%, 97%

F. CD4+ Lymphocytes — CD45RA PE vs CD62L FITC; 1%, 0.3%, 1%

Flores et al
Figure 2

37

A.

DSB 5' of D$_\beta$

DSB 3' of D$_\beta$

TCR rearrangement

linker ligation

nested PCR

PCR products

409 bp

492 bp

B.

1 2 3 4 5 6 7 8 9 10 11 12 13 14 15 16 17 18

- 900 bp
- 800
- 500
- 400

D-J →
V-DJ →

C.

D-J — 492 bp

V-DJ — 409

control — 956
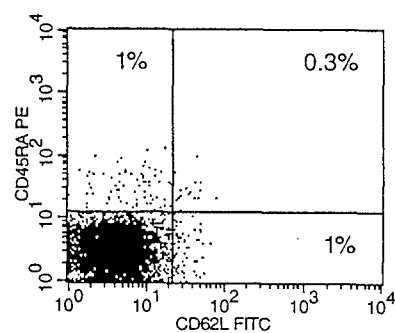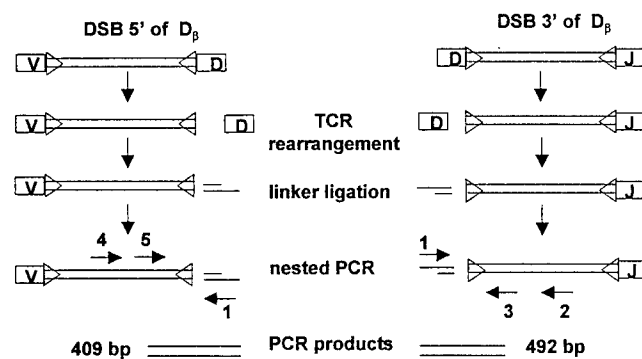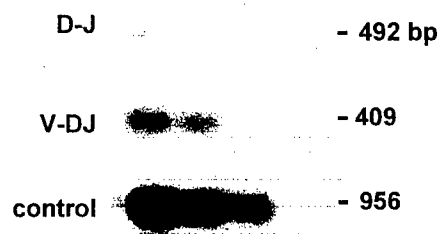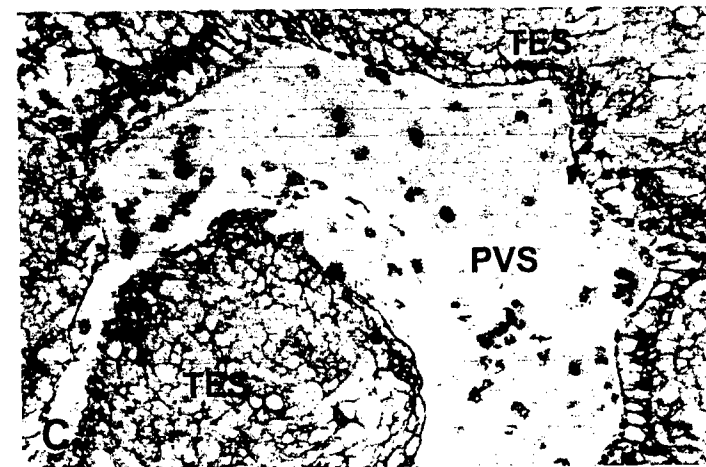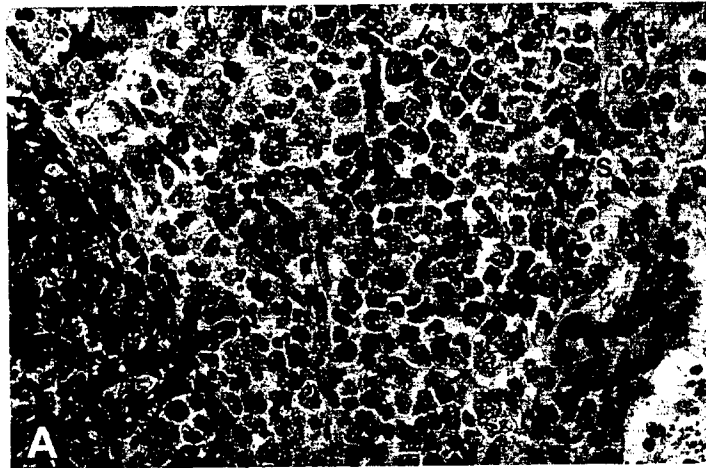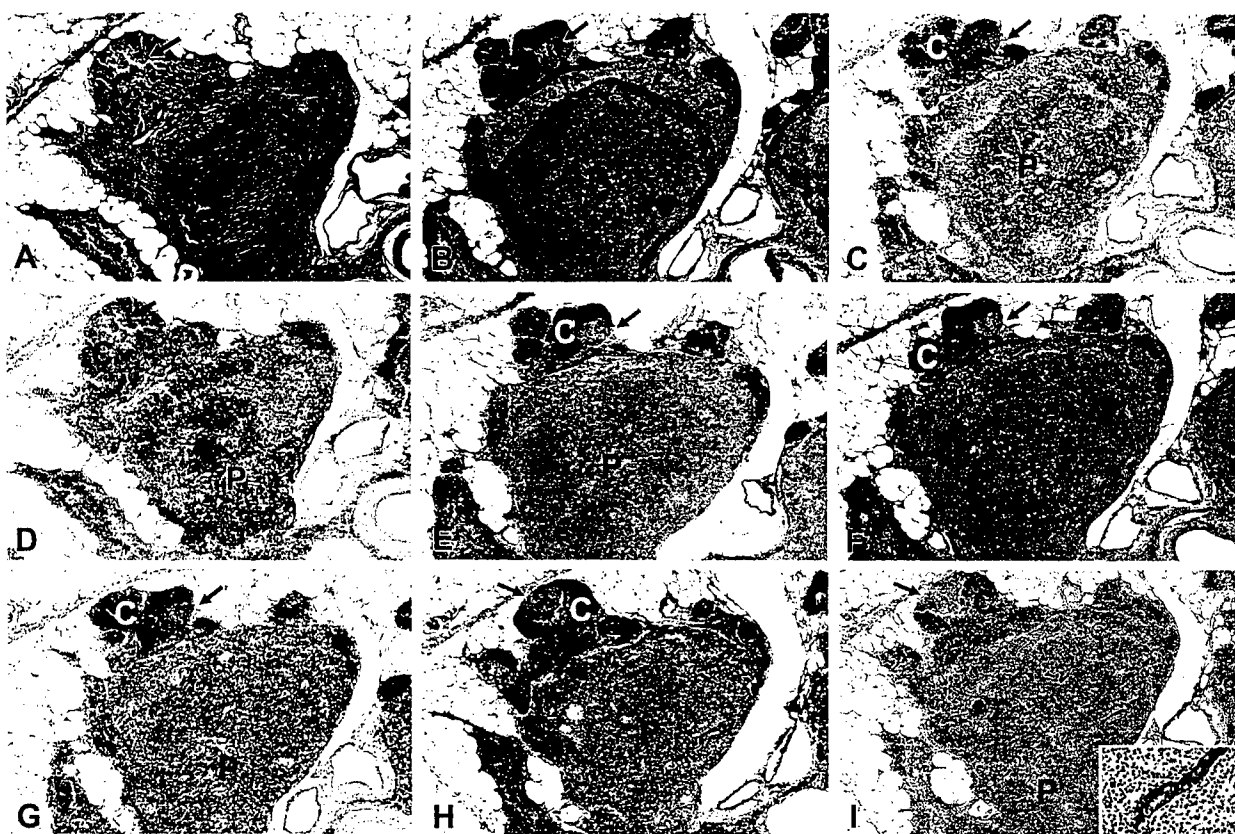
Flores et al
Figure 3

38

Flores et al
Figure 4

Flores et al
Figure 5

ANALYSIS OF THE HUMAN PERIVASCULAR SPACE DURING AGING

Kristina G. Flores, Jie Li, Gregory D. Sempowski, Barton F. Haynes, and Laura P. Hale. Duke University Medical Center, Durham, NC

The perivascular space of human thymus increases in volume during aging as thymopoiesis declines. Understanding the composition of the perivascular space is thus vital to understanding mechanisms of thymic atrophy. We have analyzed 87 normal and 31 myasthenia gravis thymus tissues from newborn to 78 years using immunohistologic and molecular assays. We confirmed that although thymic epithelial space volume decreases progressively with age, thymopoiesis with active T-cell receptor gene rearrangement continued normally within the thymic epithelial space into late life. Hematopoietic cells present in the adult perivascular space include T-cells, B cells, and monocytes. Eosinophils are prominent in perivascular space of infants $\leq$ age 2. Perivascular space of both normal adult and myasthenia gravis thymus contains mature single positive (CD1a^{-}, CD4^{+} or CD8^{+}) T lymphocytes that express CD45RO, including clusters of T-cells expressing the TIA-1 cytotoxic granule antigen, suggesting a peripheral origin. Peripheral blood mononuclear cells bind *in vitro* to MECA-79^{+} high endothelial venules present in the perivascular space, suggesting a mechanism for the recruitment of peripheral cells to thymic perivascular space. Thus in both normal subjects and myasthenia gravis patients, thymic perivascular space may be a compartment of the peripheral immune system that is not directly involved in thymopoiesis.

DEPARTMENT OF THE ARMY
US ARMY MEDICAL RESEARCH AND MATERIEL COMMAND AND FORT DETRICK
810 SCHRIEDER STREET, SUITE 218
FORT DETRICK, MARYLAND 21702-5000

REPLY TO
ATTENTION OF:

MCMR-RMI-S   (70-1y)   17 Oct 01

MEMORANDUM FOR Administrator, Defense Technical Information
Center (DTIC-OCA), 8725 John J. Kingman Road, Fort Belvoir,
VA 22060-6218

SUBJECT: Request Change in Distribution Statement

1.   The U.S. Army Medical Research and Materiel Command has
reexamined the need for the limitation assigned to technical
reports written for grants.   Request the limited distribution
statements for the Accession Document Numbers listed at enclosure
be changed to "Approved for public release; distribution
unlimited."   These reports should be released to the National
Technical Information Service.

2.   Point of contact for this request is Ms. Judy Pawlus at
DSN 343-7322 or by e-mail at judy.pawlus@det.amedd.army.mil.

FOR THE COMMANDER:

                                 PHYLIS M. RINEHART
                                 Deputy Chief of Staff for
                                     Information Management

Enclosure